AIP Journal of Applied Physics

Heating effects in nanofocusing metal wedges

Shiaw Juen Tan and Dmitri K. Gramotnev

Citation: Journal of Applied Physics **110**, 034310 (2011); doi: 10.1063/1.3615843

View online: http://dx.doi.org/10.1063/1.3615843

View Table of Contents: http://scitation.aip.org/content/aip/journal/jap/110/3?ver=pdfcov

Published by the AIP Publishing

Heating effects in nanofocusing metal wedges

Shiaw Juen Tan[1,a)] and Dmitri K. Gramotnev[2,b)]
[1]*Applied Optics and Nanotechnology Program, Faculty of Science and Technology, Queensland University of Technology, GPO Box 2434, Brisbane, QLD 4001, Australia*
[2]*Nanophotonics Pty Ltd, GPO Box 786, Brisbane, QLD 4035, Australia and Institute for Technology and Innovation, University of Southern Denmark, Niels Bohrs Alle 1, DK 5230, Odense M, Denmark*

(Received 1 June 2011; accepted 15 June 2011; published online 8 August 2011)

This paper investigates theoretically and numerically local heating effects in plasmon nanofocusing structures with a particular focus on the sharp free-standing metal wedges. The developed model separates plasmon propagation in the wedge from the resultant heating effects. Therefore, this model is only applicable where the temperature increments in a nanofocusing structure are sufficiently small not to result in significant variations of the metal permittivity in the wedge. The problem is reduced to a one-dimensional heating model with a distributed heat source resulting from plasmon dissipation in the metal wedge. A simple heat conduction equation governing the local heating effects in a nanofocusing structure is derived and solved numerically for plasmonic pulses of different lengths and reasonable energies. Both the possibility of achieving substantial local temperature increments in the wedge (with a significant self-influence of the heating plasmonic pulses), and the possibility of relatively weak heating (to ensure the validity of the previously developed nanofocusing theory) are demonstrated and discussed, including the future applications of the obtained results. Applicability conditions for the developed model are also derived and discussed. © *2011 American Institute of Physics*. [doi:10.1063/1.3615843]

I. INTRODUCTION

One of the major research directions in modern nanophotonics and nano-optics is related to focusing of light into regions with dimensions as small as a few nanometers, i.e., far beyond the diffraction limit of light. This is called nanofocusing of light. Nanofocusing has a wide range of applications, including high-resolution near-field microscopy, nano-optical sensors and detection techniques, and new approaches for effective delivery of light energy to nanoscale structures such as quantum dots, single molecules, nano-optical devices, etc.[1–12] One of the most common approaches to nanofocusing of light is based on strongly localized surface plasmons in tapered metallic waveguides, such as sharply tapered metal rods,[12–18] tapered gaps and V-shaped grooves in metals,[19–23] dielectric conical and pyramidal tips covered in metal films,[2,6,8,13,14,17,20,24,25] and sharp metal wedges and tapered sections of metal films on dielectric substrates.[23,26–31]

However, one of the important practical and physical aspects of plasmon nanofocusing—the possibility of significant local heating of nanofocusing structures caused by dissipation of plasmon energy in the metal (Refs. 32 and 33)—has received only limited attention so far. At the same time, this effect may lead to significant alteration of material properties of nanofocusing structures, self-influence of focused plasmons, and even rapid destruction of the structure, especially near the tip where the energy dissipation rates can be the greatest.

The aim of this paper is to theoretically investigate the heating effects in freestanding nanofocusing sharp metal wedges. Critical regimes for achieving high temperature near the tip of the wedge are determined and discussed from two different perspectives. On the one hand, we will determine and characterize the typical nanofocusing regimes that do not lead to significant heating effects, so that the previous nanofocusing theory[13,19,21,26,28,30,34] remains valid. On the other hand, we will also determine and analyze the conditions for the opposite situation where heating effects are rather rapid and strong, so that they can be used for rapid heating and targeted delivery of the thermal energy to the nanoscale structures. This may be especially important for applications of nanofocusing in nonlinear plasmonics, nanobiotechnology, and optical methods of diagnostics of living cells.

II. APPROXIMATIONS AND METHODS

A. Geometrical optics approximation

Consider a sharply tapered metal wedge with the taper angle γ and permittivity $\varepsilon_m = e_1 + ie_2$ ($e_1 < 0$, $e_2 > 0$), surrounded by vacuum or air ($\varepsilon_d = 1 < |e_1|$)—Fig. 1. Only the symmetric film plasmons (with the symmetric charge distribution across the wedge) can experience nanofocusing in a tapered wedge.[26,28] Therefore, in this paper, we consider plasmons with this particular symmetry, propagating normally toward the wedge tip (Fig. 1).

The plasmon propagation in the wedge can be analyzed in the geometrical optics approximation (GOA) if the taper angle is sufficiently small, such that the variations of the plasmon wave number $q = q_1 + iq_2$ within one plasmon wavelength are negligible[21,26,28,30]:

$$\left|d(q_1^{-1})/dy\right| \ll 1, \tag{1}$$

a)Author to whom correspondence should be addressed. Electronic mail: sj.tan@qut.edu.au.
b)Electronic mail: d.gramotnev@nanophotonics.com.au.

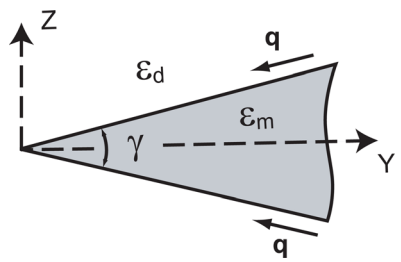

FIG. 1. (Color online) Tapered metal wedge with metal permittivity ε_m surrounded by vacuum with the permittivity $\varepsilon_d = 1$. A symmetric film plasmon with the wave vector $\mathbf{q}$ propagates in the direction normal to the tip of the wedge.

where we assume that the plasmon dissipation is weak: $q_2 \ll q_1$, and the y axis is antiparallel to the direction of plasmon propagation (Fig. 1).

In the GOA approximation, the dissipation of the plasmon energy in the metal wedge at any distance from the tip can be determined assuming that the plasmon propagates in a uniform metal film of thickness that is equal to the local thickness of the metal wedge at the considered point.[26,28] Because dissipation of the plasmon energy occurs through its transformation into heat, the amount of energy dissipated at a given distance from the tip of the wedge is equal to the heat discharge (heat source) at this distance.

B. One-dimensional heat conduction approximation

Significant nanofocusing effect, field localization, and enhancement typically occur at local thicknesses of the wedge that are of the order of, or less than, the skin depth in the metal.[12,26,28] Therefore, the thermal effects will also mainly be considered at such small local wedge thicknesses, especially because this is also the case where the heating effects are expected to be the strongest. In this case, we can assume that the heat source (due to dissipation of the symmetric plasmon in the metal) and the temperature are uniform across the wedge (i.e., z independent, Fig. 1). There are two reasons supporting this approximation.

First, at local wedge thicknesses h that are of the order of, or less than, the skin depth:

$$h \lesssim 2\alpha^{-1}, \tag{2}$$

where α is the reciprocal penetration depth of the symmetric plasmon into the metal, the electric field in the symmetric plasmon in the metal is approximately uniform across the wedge. The factor of 2 is present on the right-hand side of Eq. (2) because the plasmon field penetrates into the wedge from both its sides. If condition (2) is satisfied, the heat source caused by dissipation of the symmetric plasmon in the wedge is approximately uniform (as well as the temperature distribution) across the wedge in the z direction (Fig. 1).

Second, even if condition (2) is not satisfied, in thin and sharp wedges (with the taper angles around a few degrees) that are typically used for plasmon nanofocusing,[26,28] thermal equilibrium across the wedge is established much faster than along the wedge, and any heat source nonuniformities (caused by the plasmon decay into the metal) across the wedge are efficiently smoothed out. This occurs if the other two conditions are satisfied:

$$h \ll 2\left(2\sqrt{\frac{\kappa\tau}{c_p\rho}} + \alpha^{-1}\right), \tag{3a}$$

$$h \ll l, \tag{3b}$$

where κ is the thermal conduction coefficient of the metal, τ is the duration of the plasmonic pulse, c_p is the specific heat of the metal per unit mass at constant pressure, ρ is the density of the metal, and l is the typical distance along the wedge within which the temperature varies significantly in the absence of heat conduction (i.e., where $\kappa = 0$).

Condition (3a) represents the situation where the time that it takes for the heat to diffuse across the wedge (to ensure approximately uniform distribution of the temperature across the wedge) is much smaller than the pulse duration. The factor 2 appears in front of the parentheses because both the wedge sides are heated equally by the symmetric plasmon, which makes the heat diffuse toward the middle of the wedge simultaneously from both its sides. Condition (3b) ensures that during the time required to establish a uniform temperature and heat distribution across the wedge (i.e., along the z axis, Fig. 1), heat conduction does not have enough time to noticeably redistribute the heat along the wedge (i.e., along the y axis, Fig. 1).

Under conditions (2) or (3a) and (3b), i.e., reasonably close to the tip, heat conduction in the nanofocusing wedge can approximately be reduced to a one-dimensional problem with a distributed heat source that is uniform across the wedge, i.e., z independent. Note that this approximation is correct only if the wedge is surrounded by vacuum or air (or any other material whose thermal conduction can be neglected). We also assume that there are no significant heat radiation losses from the heated wedge, which is correct for the not very high temperatures considered.

C. One-dimensional heat conduction equation

In the discussed approximation, the wedge can be replaced by an effective medium with the y-dependent thermal conductivity:

$$\kappa_{\text{eff}} = 2\kappa y \tan(\gamma/2), \tag{4}$$

where γ is the taper angle (Fig. 1). In this case, the one-dimensional Fourier's law of heat conduction can be written as

$$Q = -\kappa_{\text{eff}}\partial T/\partial y, \tag{5}$$

where Q is the heat flow in the wedge (or the heat flux in the effective medium) along the y axis (Fig. 1), calculated per unit length of the x axis.

Energy conservation gives

$$\partial Q/\partial y = Q_g - \rho_{\text{eff}} c_p \partial T/\partial t, \tag{6}$$

where Q_g is the heat source in the wedge: $Q_g = dW/dy$, dW is the amount of heat generated by the surface plasmon within

the section of the wedge of length dy per 1 s and per unit length along the x axis, and

$$\rho_{\text{eff}} = 2\rho y tan(\gamma/2). \tag{7}$$

Substituting Eq. (5) in Eq. (6), we obtain:

$$\frac{\partial}{\partial y}\left[-\kappa_{\text{eff}}(y)\frac{\partial T}{\partial y}\right] = Q_g - \rho_{\text{eff}}(y)c\frac{\partial T}{\partial t}. \tag{8}$$

Taking into account Eqs. (4) and (7) gives

$$2\kappa\ \tan(\gamma/2)\frac{\partial T}{\partial y} + 2\kappa y\ \tan(\gamma/2)\frac{\partial^2 T}{\partial y^2} = Q_g + 2\rho y c\ \tan(\gamma/2)\frac{\partial T}{\partial t}. \tag{9}$$

Equation (9) is the one-dimensional thermal conduction equation describing temperature evolution in a nanofocusing metal wedge. It is different from the conventional parabolic thermal conduction equation by the presence of the additional term on the left-hand side with the first-order derivative of the temperature with respect to y. This term can be neglected only if it is much smaller than the term with the second-order derivative of T with respect to y:

$$\left|\frac{\partial T}{\partial y}\right| \ll \left|y\frac{\partial^2 T}{\partial y^2}\right|. \tag{10}$$

It is clear that if the derivative of the temperature with respect to the y coordinate is not equal to zero near the tip of the wedge, then condition (10) is not satisfied at small values of y. In this case, this condition can only be satisfied at sufficiently large distances from the tip. Therefore, the correct analysis of thermal effects near the tip of a nanofocusing wedge requires the analysis of the derived equation (9), rather than the conventional parabolic equation of heat conduction.

The term with the first-order y derivative of T on the left-hand side of Eq. (9) is physically related to the fact that relative variations of the local wedge thickness within a given distance dy increase with decreasing distance from the tip. As a result, the difference between the values of κ_{eff} at the wedge cross-sections y and $y+dy$ increases with decreasing y, i.e., with decreasing distance to the tip. This means increased difference between the heat flows through these cross sections, which is caused by varying κ_{eff}. This is only when condition (10) is satisfied that this effect can be neglected and κ_{eff} in Eq. (8) can be assumed to be approximately constant.

Equation (8) is the general equation describing one-dimensional heat conduction and temperature evolution in any medium with continuously varying thermal conductivity, density, and/or specific heat. For example, Eq. (8) is also correct for the consideration of heating effects in a sharp metal cone with plasmon nanofocusing, which is surrounded by vacuum or air. However, in this case, the equations for the effective thermal conductivity [Eq. (4)] and effective density [Eq. (7)] should, respectively, be replaced by the following:

$$\kappa_{\text{eff}} = 4\pi\kappa y^2\ \tan^2(\gamma/2), \tag{11}$$

$$\rho_{\text{eff}} = 4\pi\rho y^2\ \tan^2(\gamma/2), \tag{12}$$

where γ is the taper angle of the metal cone. Later in this paper we will focus on the numerical analysis of Eq. (9) for nanofocusing metal wedges.

D. Further approximations and boundary conditions

In our analysis, we will mainly focus on the determination of temperature variations in a wedge within short time intervals (typically ~0.1–10 ns). On the one hand, this will give the rates of temperature increase in nanofocusing wedges on the indicated time scale during nanofocusing of cw plasmons. On the other hand, these temperature variations will approximately correspond to the heating effects during nanofocusing of rectangular plasmonic pulses with the respective duration of ~0.1–10 ns. However, the conducted analysis is only an approximation for the actual plasmonic pulses, as it neglects their spectral composition (which is reasonable at the considered pulse lengths) and any effects associated with the propagation of the front and rear of the pulse along the wedge. The latter assumption is typically well satisfied for pulses whose spatial length is much larger than the length of the nanofocusing wedge:

$$\tau \gg l_{\text{opt}} n_{\text{eff}}/c, \tag{13}$$

where c is the speed of light, n_{eff} is the typical effective refractive index for the localized symmetric plasmon in the wedge, and l_{opt} is the optimal length of the wedge (which is typically ~1 μm).[26,28] Because the right-hand side of condition (13) is $\sim 10^{-14}$ s for nanofocusing wedges, this condition is well satisfied for picosecond and nanosecond pulses.

We also assume that the metal permittivity does not change as the wedge temperature increases. Obviously, such an assumption is only correct if the temperature variations are not very large. If this condition is not satisfied, the imaginary part of the metal permittivity typically increases with increasing temperature, which enhances dissipative effects (see the following for the analysis of the typical temperature distribution patterns depending on values of the imaginary part of the metal permittivity).

Because in the approximation of continuous electrodynamics with local response nanofocused symmetric plasmons experience infinite enhancement and localization at an infinitely sharp tip of a wedge, the numerical finite-difference time-domain analysis of the one-dimensional heat conduction equation was conducted within a computational window whose boundary was at a finite (though small) distance from the tip. At this boundary, i.e., at the computational point that is the closest to the tip, we assume the second-order derivative of the temperature with respect to the y coordinate to be the same as at the next closest point:

$$\frac{(T_1 - T_2) - (T_2 - T_3)}{\Delta y^2} = \frac{(T_2 - T_3) - (T_3 - T_4)}{\Delta y^2}, \tag{14}$$

where $T_{1,2,3,4}$ are the temperature values at the first, second, third, and fourth computational points from the boundary of the computational window near the tip of the wedge, and Δy

is the spatial separation between the neighboring computational points. This boundary condition near the tip of the wedge ensures the approximately correct heat flow into the computational window from the regions closer to the tip, thus allowing solution of the problem in the approximation of the continuous electrodynamics, local dielectric response, and infinitely sharp tip of the wedge (with no reflections of the plasmon from the tip).

The boundary condition at the other edge of the computational window, i.e., far away from the tip, is not important as this boundary can be moved arbitrarily far from the region where temperature distribution is sought, so that this condition has a negligible influence on the calculation results within the region of interest.

III. ZERO THERMAL CONDUCTIVITY

The simplest situation occurs where heat conduction along the wedge (i.e., along the y axis—Fig. 1) is assumed to be zero. This approximation adequately describes the situation where the temporal length of a plasmonic pulse or the time interval within which the temperature variations are determined is

$$\tau \ll \frac{l^2 c_p \rho_{\text{eff}}}{4\kappa_{\text{eff}}}, \tag{15}$$

where l is the distance along the wedge (along the y axis, Fig. 1) within which the temperature changes significantly.

Let us assume that condition (15) is satisfied and the metal wedge has a uniform initial temperature of 20 °C. In this case, the energy released at each point of the metal wedge does not have enough time to be redistributed along the wedge by means of heat conduction, and thus causes only local temperature to increase. The resultant typical temperature distributions in the nanofocusing wedges are presented in Fig. 2 for different structural and material parameters.

It can be seen from Fig. 2 that the typical temperature distributions along the metal wedge are of two distinct types depending on the level of dissipation losses. If the dissipation

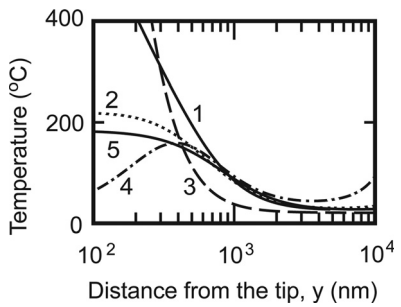

FIG. 2. Typical temperature distributions along the metal wedges with the taper angles $\gamma = 2°$ (curves 1–4), and $\gamma = 1.5°$ (curve 5), at the vacuum wavelength $\lambda_{\text{vac}} = 632.8$ nm and zero thermal conductivity $\kappa_{\text{eff}} = 0$. The metal permittivities are: (1, 5) $\varepsilon_m = -9.3 + 1.12i$; (2) $\varepsilon_m = -9.3 + 1.52i$, (3) $\varepsilon_m = -16 + i$, (4) $\varepsilon_m = -16 + 8i$. The real parts of the metal permittivities correspond to gold (Refs. 35 and 36) (curves 1, 2, and 5; $\rho = 19320$ kg/m^3, $c_p = 128$ kJ/kg °C) and silver (Refs. 35 and 36) (curves 3 and 4; $\rho = 10490$ kg/m^3, $c_p = 235$ kJ/kg °C). The energy of the plasmon pulses for all the curves was assumed to equal 10 μJ/m (per 1 m of the x axis) at the optimal distance l_{opt} from the tip of the wedge (Ref. 26), i.e., at the point where the plasmon amplitude is minimal.

is not too strong, i.e., e_2 is smaller than a critical value e_{2c}, the temperature increases rather monotonically and significantly toward the tip of the wedge (curves 1 and 3 in Fig. 2). This can be explained by the following three mechanisms.

First, as the symmetric plasmon propagates toward the tip of the metal wedge, it experiences progressively increasing localization near the wedge and reduction of its group and phase velocities.[16,26,28] As a result, a greater fraction of the plasmon energy propagates within the metal, which leads to stronger dissipative losses and associated heating effects near the tip. Second, as the plasmon propagates toward the tip of the wedge, it experiences strong local field enhancement.[16,26] As a result, the plasmon field amplitude in the metal increases, which also leads to an enhancement of local dissipative effects in the metal, and thus to an increased rate of local heating. Third, as the plasmon propagates toward the tip, the increased release of the heat energy (related to the two above-mentioned mechanisms) occurs in progressively thinner sections of the metal wedge. This means that the amount of the material (metal) that is heated by the thermal energy release caused by plasmon dissipation in the wedge reduces with approaching the wedge tip, which means even higher local temperatures in the considered approximation of zero heat conduction.

However, this typical heating pattern occurs only where dissipation is not too strong, so that a significant amount of plasmon energy can reach the regions in the immediate proximity of the tip of the wedge. If dissipation in the metal is significantly increased, i.e., if $e_2 > e_{2c}$, then the temperature initially increases with reducing distance to the tip, goes through a maximum, and then monotonically decreases in the immediate proximity to the tip (curve 4 in Fig. 2). This pattern of the temperature distribution is explained by the fact that strong dissipation in the metal (large values of e_2) results in a rapid reduction of the plasmon energy as it propagates toward the tip of the wedge. As a result, the amount of plasmon energy reaching the regions near the tip of the wedge is drastically reduced, resulting in a significant reduction of local heating (and thus reduction in temperature—curve 4 in Fig. 2).

It follows from here that there is a critical regime of nanofocusing where the local temperature in the wedge reaches a maximum in the form of a plateau at the tip of the wedge (curves 2 and 5 in Fig. 2). This critical regime corresponds to a critical value of dissipation $e_2 = e_{2c}$ in the metal, which should obviously depend upon taper angle γ of the wedge. The analysis of the obtained numerical results suggests that the critical imaginary part e_{2c} of the metal permittivity in the wedge can be related to the material and geometrical parameters of the structure by means of the following simple empiric equation:

$$e_{2c} = e_1^2 \gamma / (\vartheta \varepsilon_d), \tag{16a}$$

where the empiric constant $\vartheta \approx 113.8$, and ε_d is the permittivity of the dielectric medium surrounding the wedge (in the considered case this medium is vacuum: $\varepsilon_d = 1$).

Equation (16a) is easy to understand from a physical point of view. Increasing magnitude of the real part of the metal permittivity e_1, or reducing the dielectric permittivity of the surrounding medium, results in a decreasing fraction

of the plasmon energy propagating within the metal wedge. This leads to a decrease of the overall plasmon dissipation, and thus shifts the temperature distribution toward the first distinct pattern with the monotonic increase of the temperature toward the tip of the wedge (curves 1 and 3 in Fig. 2). This means that the critical value of the imaginary part e_{2c} of the metal permittivity must increase, which also follows from Eq. (16a). Increasing taper angle γ also results in reducing the overall dissipative losses in the metal wedge.[26,28] As a result, increasing γ must also shift the temperature distribution toward the first distinct pattern and also result in increasing e_{2c}—again in agreement with Eq. (16a).

It can also be said that, for the fixed material parameters of the structure, Eq. (16a) can be rewritten as an equation determining the critical angle γ_c:

$$\gamma_c = e_2 \vartheta \varepsilon_d / e_1^2. \tag{16b}$$

If the wedge taper angle $\gamma > \gamma_c$, then the temperature in the wedge monotonically increases toward the tip (the first distinct pattern of the temperature distribution—curves 1 and 3 in Fig. 2). If the taper angle $\gamma < \gamma_c$, then the temperature in the wedge goes through a maximum at some distance from the tip and then starts to decrease closer to the tip (the second distinct pattern of the temperature distribution—curve 4 in Fig. 2).

As demonstrated by Fig. 2, the achievable temperature variations and local heating significantly depend on material and geometrical parameters of the structure. The typical variations of the achievable local temperatures vary by hundreds of degrees. Somewhat counterintuitive is the fact that larger local temperatures can be achieved at weaker dissipation in the metal, because in this case larger fraction of the plasmon energy can reach the regions in the immediate proximity to the tip, where local rates of dissipative losses are the largest and the amount of the material to be heated is the smallest.

The presented distinct patterns and typical temperature variations in a nanofocusing metal wedge have so far been considered in the approximation of zero thermal conductivity (i.e., at $\kappa_{\text{eff}} = 0$).

IV. NONZERO THERMAL CONDUCTIVITY

The results obtained in the previous section are valid only for sufficiently short plasmonic pulses [condition (15)]. If condition (15) is not satisfied, heat conduction in the y direction results in a significant temperature redistribution along the wedge, and the numerical solution of Eq. (9) is required. Similar to the previous case, the metal wedge is assumed to have a uniform initial temperature of 20 °C. Figure 3(a) shows the temperature distributions along a gold metal wedge surrounded by vacuum for several different lengths of the plasmonic pulse. In particular, it can be seen that, as the pulse length is increased, the temperature maximum at around ~600 nm from the tip is smoothed out by the heat transfer, leading to a significant temperature redistribution near the tip of the wedge [compare the curves in Fig. 3(a)].

Figure 3(b) illustrates the effect of the taper angle and dielectric permittivity of the metal on the obtained typical temperature distributions in a nanofocusing metal wedge. For example, increasing taper angle results in increasing temperature near the tip [compare curves 1 and 2 in Fig. 3(b)]. This is because increasing taper angle results in decreasing the effect of dissipation in the metal (as the plasmon needs to propagate smaller distance toward the tip). Therefore, more plasmon energy reached the regions in the immediate proximity to the tip, where dissipative losses (and thus the heating effects) are the strongest. Similarly, increasing the real part of the metal permittivity and decreasing its imaginary part also results in decreased dissipation losses in the metal, and again a larger fraction of the plasmon energy reaches the region near the tip with the strongest dissipation, thus enhancing local heat discharge in the vicinity of the tip. These results once again highlight the somewhat counterintuitive finding of this analysis that stronger heating effects near the tip of a nanofocusing wedge occur for the wedges with weaker dissipation in the metal. In the presence of heat conduction, this effect is reduced by the occurring heat redistribution along the wedge, but it is typically quite significant for the structures typically required for plasmon nanofocusing [Fig. 3(b)].

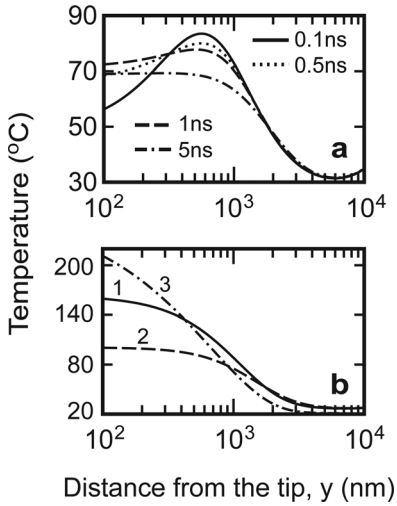

FIG. 3. (a) Temperature distributions along the gold wedges (Refs. 35 and 36) with the permittivity $\varepsilon_m = -9.3 + 1.52i$ and taper angle $\gamma = 1.5°$ for four different lengths of the heating plasmonic pulses; $\rho = 19320$ kg/m^3, $c_p = 128$ kJ/kg °C, $\kappa = 315$ W/m °C. (b) Temperature distributions along the gold (Refs. 35 and 36) (curves 1 and 2; $\rho = 19320$ kg/m^3, $c_p = 128$ kJ/kg °C, $\kappa = 315$ W/m °C) and silver (Refs. 35 and 36) (curve 3; $\rho = 10490$ kg/m^3, $c_p = 235$ kJ/kg °C, $\kappa = 428$ W/m °C) metal wedges for $\gamma = 2°$ (curves 1 and 3) and $\gamma = 1.5°$ (curve 2), at $\lambda_{\text{vac}} = 632.8$ nm and the pulse length $\tau = 5$ ns. The metal permittivities (Ref. 36) for gold and silver are $\varepsilon_m = -9.3 + 1.12i$ and $\varepsilon_m = -16 + i$, respectively. The energy of the plasmon pulses for all the curves was assumed to equal 10 μJ/m (per 1 m of the x axis) at the optimal distance l_{opt} from the tip of the wedge (i.e., at the point where the plasmon amplitude is minimal—Ref. 26).

Another important aspect demonstrated by Fig. 3(b) is related to the rate of temperature decay away from the tip of a nanofocusing wedge. This rate determines the degree of localization of the heat discharge near the tip of the structure: the larger the rate of the temperature decay, the stronger the localization of the heat discharge near the tip. Thus, increasing taper angle and decreasing dissipation in the metal result in increasing localization of the heat discharge near the tip [Fig. 3(b)]. This aspect will be important for the design of efficient structures for highly targeted and localized delivery of the heat energy to nanoscale structures. For example, to ensure strong and highly localized heat discharge on the

nanoscale, we need to ensure that the increase of the temperature occurs within a region with as small dimensions as possible. From this point of view, it will be beneficial to use nanofocusing structures with the least dissipative effects in the metal—only in this case is the local heat discharge near the tip maximally localized [Fig. 3(b)].

Importantly, this tendency is rather general and will typically also apply to nanofocusing structures in a heat-conducting environment, where the tip is surrounded by a dielectric medium, for example, in water, or in a biological specimen, etc. Certainly, the typical pulse lengths at which the considered highly localized heat discharge and subsequent heating effects take place will be different from (smaller than) those obtained earlier in this paper for a free-standing wedge in vacuum or air. At the same time, the general tendencies and typical patterns will remain the same, as long as the pulse length is small enough to prevent heat transfer into the environment within distances significantly larger than those typical for the heating patterns in the free-standing wedges (Figs. 2 and 3).

Because the heating effect in the nanofocusing structures are typically the strongest near the tip (Figs. 2 and 3), it is useful to further investigate the temperature dependencies near the tip on taper angle and vacuum wavelength (frequency) of the propagating plasmon. Figure 4(a) shows such dependencies on taper angle at a small distance from the tip of the wedge, corresponding to the local wedge thickness $h=2$ nm, for the two silver wedges with different levels of dissipation (imaginary parts of the metal permittivity). Both the curves display significant temperature maximums demonstrating the existence of a *T*-optimal taper angle that increases with increasing dissipation in the metal [compare curves 1 and 2 in Fig. 4(a)]. The terminology "*T*-optimal"is used here to distinguish the optimal taper angle at which the temperature near the tip is maximal from the optimal taper angle resulting in the maximal local field enhancement near the tip.[13,17]

If the taper angle is very small (smaller than the *T*-optimal angle), then the plasmon travels large distances before reaching the regions near the tip, which means that its energy has been significantly diminished, thus leading to lower heat discharge and reduced temperatures near the tip [Fig. 4(a)]. If the taper angle is larger than the *T*-optimal angle, more energy of the plasmon reaches the regions near the tip, which should lead to larger local heat discharge. However, simultaneously, the efficiency of heat conduction and its transfer away from the tip also increases with increasing taper angle, as κ_{eff} increases more rapidly away from the tip with increasing γ [Eq. (4)], and the temperature gradient also increases due to more rapidly changing plasmon propagation parameters. The competition of these two opposing mechanisms results in a *T*-optimal taper angle at which the temperature near the tip is maximal [Fig. 4(a)].

Similarly, Fig. 4(b) shows that there is a *T*-optimal wavelength at which the temperature near the tip of a nanofocusing wedge is maximal. Increasing taper angle results in decreasing *T*-optimal wavelength (increasing optimal frequency) of the plasmon at which the temperature maximum is achieved near the tip (compare curve 1 with curve 3 and curve 2 with curve 4).

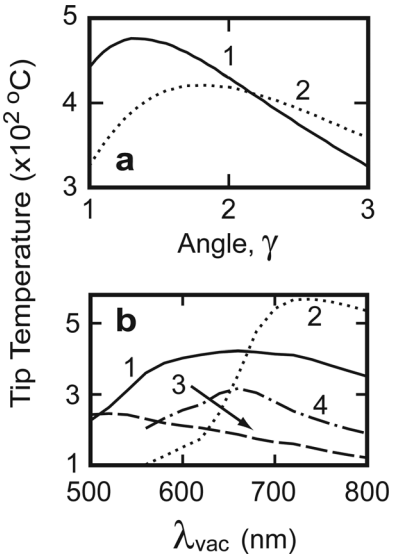

FIG. 4. (a) The dependencies of temperature on taper angle of the silver (Refs. 35 and 36) wedges ($\rho=10490$ kg/m^3, $c_p=235$ kJ/kg °C, $\kappa=428$ W/m °C, $\lambda_{\text{vac}}=632.8$ nm, and $\tau=2$ ns) at the points where the local thickness of the metal wedge $h=2$ nm for the two different values of the metal permittivity (1) $\varepsilon_m=-16+i$, and (2) $\varepsilon_m=-16+1.5i$. The energy of the plasmonic pulses at the optimal distance l_{opt} from the tip is 10 μJ/m. (b) The dependencies of temperature on plasmon wavelength λ_{vac} in silver (Ref. 35) (curves 1 and 3; $\rho=10490$ kg/m^3, $c_p=235$ kJ/kg °C, $\kappa=428$ W/m °C) and gold (Ref. 35) (curves 2 and 4; $\rho=19320$ kg/m^3, $c_p=128$ kJ/kg °C, $\kappa=315$ W/m °C) wedges with the taper angles $\gamma=2°$ (curves 1 and 2) and 5° (curves 3 and 4) at the points where the local thickness of the metal wedge $h=2$ nm. The pulse length $\tau=2$ ns, the frequency-dependent permittivities of the metal are taken from Ref. 36, and the energy of the plasmonic pulse is equal to 10 μJ at the fixed distances of 2810 nm (curve 1), 1750 nm (curve 2), 1410 nm (curve 3), and 1130 nm (curve 4) from the tip of the wedge; these distances correspond to the optimal distances (optimal wedge lengths—Ref. 26) l_{opt} at $\lambda_{\text{vac}}=632.8$ nm.

V. CONCLUSIONS

The results obtained in this paper demonstrate that both the regimes of nanofocusing—with and without strong heating effects in a sharp metal wedge—can be achieved for reasonable structural and material parameters and an appropriate reasonable choice of the energy and length of the incident plasmonic pulse. Thus, on the one hand, the obtained results establish the framework for the applicability of the previously developed theory of plasmon nanofocusing in sharp metal wedges.[26,28] On the other hand, we have also demonstrated that significant local heating effects may be achieved near the tip of the wedge, so that heat energy can be released on the nanoscale within regions with dimensions as small as dozens of nanometers. This effect opens unique applications of plasmon nanofocusing related to highly targeted and fast local heating of nanostructures and their immediate environment for the investigation and testing of their local heat response and/or heat modification and local treatment of nanoscale structures and materials.

The length of the plasmonic pulse appears to be an important parameter that allows efficient manipulation and adjustment of the temperature distribution and local heating in the considered nanofocusing structures. Interesting temperature distribution patterns with a significant temperature maximum at some distance from the tip of the nanofocusing wedge are shown to exist for sufficiently small pulse lengths

and sufficiently strong dissipative effects in the metal. A somewhat counterintuitive and important outcome has been obtained demonstrating that stronger local heating near the tip of a nanofocusing structure can be achieved at weaker dissipation in the metal. Simultaneously, stronger localization of the heat discharge and local heating can also be achieved with decreasing dissipation in the metal.

Possible temperature rise by hundreds of degrees can easily be achieved in the considered structures near the tip, which raises a possibility of significant thermal self-influence of the propagating plasmons with the achievable nonlinear response within at least picoseconds. The ultimate case of such self-influence would be heat destruction of the nanofocusing structure near the tip—the effect that may place the propagating (and heating) plasmonic pulses into a radically different condition with possible major nonlinear effects and variations of their propagation parameters. Such heat destruction of the structure near the tip will be facilitated by the possibility of a significant reduction of the melting temperature of a metal in nanoscale structures. For example, for gold metal tip with thickness as small as ~2–4 nm, the melting temperature can be reduced below ~500 °C,[37,38] which is certainly within easy reach for the considered structures.

The existence of heat conducting environment around a nanofocusing wedge or any other nanofocusing structure will significantly reduce the typical plasmonic pulse lengths that are required for achieving the predicted temperature increments near the tip. However, the typical temperature distributions and the observed counterintuitive and important tendencies (including the temperature maximum near the tip of a nanofocusing wedge with sufficiently strong dissipation in the metal) will remain largely the same, as long as the thermal conductivity in the environment is much smaller than that of the metal wedge.

The obtained results of this paper will be important for the practical design of metallic nanofocusing structures, the development of new optical sensors and measurement techniques, near-field microscopy and spectroscopy, as well as the possibility of highly targeted delivery of thermal energy to regions with nanoscale dimensions, including in the nanobiophotonics (for example, to selected regions of a living cell), etc.

[1]N. Anderson, A. Bouhelier, and L. Novotny, J. Opt. A, Pure Appl. Opt. **8**, S227 (2006).
[2]A. Bouhelier, J. Renger, M. R. Beversluis, and L. Novotny, J. Microsc. **210**, 220 (2003).
[3]H. G. Frey, F. Keilmann, A. Kriele, and R. Guckenberger, Appl. Phys. Lett. **81**, 5030 (2002).
[4]F. Kielmann, J. Microsc. **194**, 567 (1999).
[5]K. Kneipp, Y. Wang, H. Kneipp, L. T. Perelman, I. Itzkan, R. Dasari, and M. S. Feld, Phys. Rev. Lett. **78**, 1667 (1997).
[6]D. Mehtani, N. Lee, R. D. Hartschuh, A. Kisliuk, M. D. Foster, A. P. Sokolov, F. Caiko, and I. Tsukerman, J. Opt. A, Pure Appl. Opt. **8**, S183 (2006).
[7]D. Molenda, G. C. des Francs, U. C. Fischer, N. Rau, and A. Naber, Opt. Express **13**, 10688 (2005).
[8]A. Naber, D. Molenda, U. C. Fischer, H. J. Maas, C. Hoppener, N. Lu, and H. Fuchs, Phys. Rev. Lett. **89**, 210801 (2002).
[9]L. Novotny, D. W. Pohl, and B. Hecht, Ultramicroscopy **61**, 1 (1995).
[10]B. Pettinger, B. Ren, G. Picardi, R. Schuster, and G. Ertl, Phys. Rev. Lett. **92**, 096101 (2004).
[11]A. V. Zayats and I. Smolyaninov, J. Opt. A, Pure Appl. Opt. **5**, S16 (2003).
[12]D. K. Gramotnev and S. I. Bozhevolnyi, Nat. Photonics **4**, 83 (2010).
[13]D. K. Gramotnev, M. W. Vogel, and M. I. Stockman, J. Appl. Phys. **104**, 034311 (2008).
[14]K. Nerkararyan, T. Abrahamyan, E. Janunts, R. Khachatryan, and S. Harutyunyan, Phys. Lett. A **350**, 147 (2006).
[15]L. Novotny and C. Hafner, Phys. Rev. E **50**, 4094 (1994).
[16]M. I. Stockman, Phys. Rev. Lett. **93**, 137404 (2004).
[17]M. W. Vogel and D. K. Gramotnev, J. Nanophotonics **2**, 021852 (2008).
[18]N. A. Issa and R. Guckenberger, Plasmonics **2**, 31 (2007).
[19]S. I. Bozhevolnyi and K. V. Nerkararyan, Opt. Lett. **35**, 541 (2010).
[20]G. C. des Francs, D. Molenda, U. C. Fischer, and A. Naber, Phys. Rev. B **72**, 165111 (2005).
[21]D. K. Gramotnev, J. Appl. Phys. **98**, 104302 (2005).
[22]D. F. P. Pile and D. K. Gramotnev, Appl. Phys. Lett. **89**, 041111 (2006).
[23]K. V. Nerkararyan, Phys. Lett. A **237**, 103 (1997).
[24]N. C. Lindquist, P. Nagpal, A. Lesuffleur, D. J. Norris, and S. H. Oh, Nano Lett. **10**, 1369 (2010).
[25]A. J. Babadjanyan, N. L. Margaryan, and K. V. Nerkararyan, J. Appl. Phys. **87**, 3785 (2000).
[26]D. K. Gramotnev and K. C. Vernon, Appl. Phys. B: Lasers Opt. **86**, 7 (2007).
[27]M. Schnell, P. Alonso-Gonzalez, L. Arzubiaga, F. Casanova, L. E. Hueso, A. Chuvilin, and R. Hillenbrand, Nat. Photonics **5**, 283 (2011).
[28]S. J. Tan and D. K. Gramotnev, J. Appl. Phys. **107**, 094301 (2010).
[29]E. Verhagen, A. Polman, and L. Kuipers, Opt. Express **16**, 45 (2008).
[30]K. C. Vernon, D. K. Gramotnev, and D. F. P. Pile, J. Appl. Phys. **101**, 104312 (2007).
[31]E. Moreno, S. G. Rodrigo, S. I. Bozhevolnyi, L. Martin-Moreno, and F. J. Garcia-Vidal, Phys. Rev. Lett. **100**, 023901 (2008).
[32]G. Baffou, R. Quidant, and C. Girard, Appl. Phys. Lett. **94**, 153109 (2009).
[33]G. Baffou, R. Quidant, and F. J. G. de Abajo, ACS Nano **4**, 709 (2010).
[34]S. Berweger, J. M. Atkin, R. L. Olmon, and M. B. Raschke, J. Phys. Chem. Lett. **1**, 3427 (2010).
[35]W. D. Callister, *Materials Science and Engineering* (Wiley, New York, 2007).
[36]E. D. Palik, *Handbook of Optical Constants of Solids* (Academic, New York, 1985).
[37]Ph. Buffat and J-P Borel, Phys. Rev. A **13**, 2287 (1976).
[38]W. H. Qi and M. P. Wang, J. Mater. Sci. Lett. **21**, 1743 (2002).